Space Science Reviews (2025) 221:92
https://doi.org/10.1007/s11214-025-01215-0

Diffuse Continuum Emission and Large Extended Sources at MeV Energies

Markus Ackermann[1] · **Denys Malyshev**[2] · **Dmitry V. Malyshev**[3]

Received: 28 March 2025 / Accepted: 5 September 2025

Abstract
Future γ-ray survey instruments, such as *COSI*, *newASTROGAM* and *AMEGO-X*, will significantly improve previous and current all-sky surveys at MeV energies. In this paper we discuss the continuum emission from the Milky Way, two prominent large extended sources, the *Fermi* bubbles and Loop I, and the extragalactic γ-ray background. We highlight the importance of measurements in the MeV to GeV energy range for understanding CR production and propagation in the Galaxy, for the determination of the nature of the *Fermi* bubbles and Loop I, and for exploring the origin of the extragalactic γ-ray background.

Keywords Diffuse gamma-ray emission · MeV gamma rays

1 Introduction

Diffuse γ-ray emission arises from various origins and on vastly different scales. It dominates the total integrated γ-ray flux in the MeV and GeV range. In contrast to line emission from positron annihilation (Johnson and Haymes 1973; Leventhal et al. 1978; Weidenspointner et al. 2008; Siegert et al. 2020) and the decay of radioisotopes, such as ^{26}Al (Diehl et al. 1995; Bouchet et al. 2015) and ^{60}Fe (Wang et al. 2007, 2020), which are also important sources of diffuse emission in our Galaxy, diffuse continuum emission arises from the interactions of non-thermal particles with radiation and matter. We focus on this continuum emission below rather than the line emission, which is discussed elsewhere in this edition.

The diffuse γ-ray emission has its origins in the solar system, the Milky Way, and the Universe beyond. Within the solar system, the most prominent sources of diffuse radiation

✉ M. Ackermann
markus.ackermann@desy.de

D. Malyshev
denys.malyshev@astro.uni-tuebingen.de

D.V. Malyshev
dmitry.malyshev@fau.de

1 Deutsches Elektronen-Synchrotron DESY, Platanenallee 6, 15738 Zeuthen, Germany

2 Institut für Astronomie und Astrophysik Tübingen, Universität Tübingen, Sand 1, 72076 Tübingen, Germany

3 Erlangen Centre for Astroparticle Physics, Nikolaus-Fiebiger-Str. 2, 91058 Erlangen, Germany

Published online: 03 October 2025

are cosmic-ray (CR) interactions with the Earth atmosphere (e.g., Kraushaar et al. 1972; Abdo et al. 2009) and the radiation field of the sun (Orlando and Strong 2008; Abdo et al. 2011). The Galactic diffuse emission is produced by the interactions of CRs with the interstellar gas (ISG) and interstellar radiation fields (ISRF). It is customary to distinguish the bulk diffuse Galactic emission (DGE) that is fueled by quasi-continuous CR production, propagtion and escape on the scale of the entire Milky Way from individual, large-scale structures that arise from transient and/or localized CR injection events (e.g., Loop I and Fermi Bubbles, see below).

The extragalactic diffuse emission, also called the extragalactic γ-ray background (EGB) is dominantly produced by faint or distant γ-ray sources that are unresolved by current instruments. Known populations of extragalactic γ-ray sources include active galactic nuclei (AGN) (Inoue et al. 2008), star-forming galaxies (Lacki et al. 2014), but also transients such as supernovae (SN), dominated by SN Type Ia (SNIa) (Clayton and Ward 1975; Watanabe et al. 1999a; Ruiz-Lapuente et al. 2016), and gamma-ray bursts (GRB) (Ajello et al. 2019). Other potential contributions to the EGB arise from CR interactions with the cosmic microwave background (CMB) (Berezinskii and Smirnov 1975) and beyond-the-standard-model (BSM) physics processes (Bergström et al. 2001; Carr et al. 2021). Due to its predominant origin from unresolved sources, the measured diffuse extragalactic emission depends on the sensitivity and angular resolution of the instrument used. We therefore use a convention here introduced in Ackermann et al. (2015a) to distinguish between the isotropic γ-ray background (IGRB) that encompasses only the diffuse extragalactic emission and the *total EGB* that includes the IGRB and all resolved extragalactic sources. The latter is independent of the instrument used to measure it and encompasses the entire extragalactic γ-ray emission from astrophysical sources.

This manuscript summarizes the current knowledge and open science questions related to the diffuse γ-ray emission in the MeV range, focusing on the Galactic and extragalactic components. Section 2 discusses the DGE. Section 3 focuses on the largest extended features of the Galactic γ-ray sky, the *Fermi* bubbles and Loop I. Section 4 discusses the extragalactic diffuse background, what is known about its origin, and the prospects for future missions to constrain the contributions of various source populations and new physics.

2 Diffuse Galactic Emission

The DGE arises from the interactions of CRs with the ISG and the ISRF via various processes, such as bremsstrahlung, inverse Compton (IC) scattering, and pion decay. Observations of the DGE play a crucial role in understanding CR propagation in the Milky Way and the interstellar medium (ISM) properties of our Galaxy. It has been observed by several generations of γ-ray telescopes, including the *OSO-3* (Kraushaar et al. 1972), *SAS-2* (Fichtel et al. 1975), *COS-B* (Bignami et al. 1975), *EGRET* (Hunter et al. 1997) and the *Fermi*-LAT (Ackermann et al. 2012c) instruments at energies above few tens of MeV. *COMPTEL* (Strong et al. 1994), *OSSE* (Skibo et al. 1997) *INTEGRAL/SPI* (Bouchet et al. 2008) and, recently, *COSI* (Karwin et al. 2023) provide measurements of the DGE in the energy range from 20 keV to few tens of MeV.

Figure 1 shows the DGE in the direction of the inner Galaxy as measured during the 2016 *COSI* balloon flight, by the *COMPTEL* instrument on the *Compton Gamma-Ray Observatory (CGRO)*, and the *Spectrometer on INTEGRAL (SPI)* in the energy range between 50 keV and 30 MeV in comparison to expectations. A common method for studying the DGE in the MeV and GeV energy regimes involves modeling the CR production and propagation in

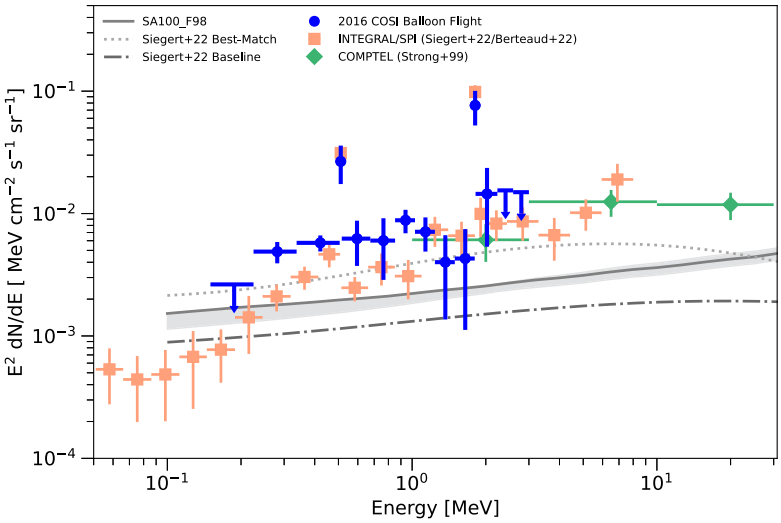

Fig. 1 Measurements of the DGE in the direction of the inner Galaxy during the 2016 *COSI* balloon flight (Karwin et al. 2023), by COMPTEL (Strong et al. 1994, 1999), and SPI (Siegert et al. 2022; Berteaud et al. 2022) in comparison to expectations (Porter et al. 2022; Siegert et al. 2022). The models do not include line emission visible in the data at 511 keV (e^+/e^- annihilation) and 1.81 MeV (^{26}Al decay). Image reproduced with permission from Karwin et al. (2023), copyright by the author(s)

the Milky Way, as well as the emission of γ rays from CR interactions with the ISG and ISRF via a propagation code, such as GALPROP (Vladimirov et al. 2011), DRAGON (Evoli et al. 2017), or PICARD (Kissmann 2014). Comparison of the model predictions with the observed DGE and local observations of primary and secondary CRs allow one to study and constrain the parameters that enter the model, such as the CR source distribution, diffusion coefficients, the roles of convection and/or re-acceleration of CRs in the interstellar medium, CR halo size (e.g., Ackermann et al. 2012c). In addition, the DGE can be used to study ISM properties, such as the ISG and ISRF distribution, and the Galactic magnetic field structure. The excess of the observed continuum DGE over predictions from CR propagation models above few hundred keV that is visible in Fig. 1 is generally attributed to contributions from unresolved γ-ray sources (Tsuji et al. 2023). However, also other contributions are possible, such as a more intense radiation field in the Galactic bulge (Porter et al. 2008; Bouchet et al. 2011) or a contribution from the annihilation of dark matter particles in the MeV mass range (Luque et al. 2025).

Figure 2 demonstrates the importance of the MeV window for constraining CR propagation. The figure shows two different models of the Galactic diffuse emission computed with GALPROP(v57) (Porter et al. 2022) in comparison to the MeV measurements of the DGE featured in Fig. 1, and measurements above 200 MeV obtained from the *Fermi*-LAT data for a different region of the sky (Ackermann et al. 2012c). Both models use the same distribution of CR sources for injecting CR (Galactic Pulsar distribution, Yusifov and Küçük 2004), and are tuned to the same set of CR observations. For CR electrons+positrons, these are the low-energy (< 50 MeV) measurements by *Voyager 1* in interstellar space (Cummings et al. 2016), and high-energy measurements by *AMS-02* (Aguilar et al. 2014) and *HESS* (Aharonian et al. 2008), both performed at or near Earth.

The first model assumes plain CR diffusion with a break in the rigidity dependence of the diffusion coefficient at 4 GV. In addition, convection of CRs is modeled with a con-

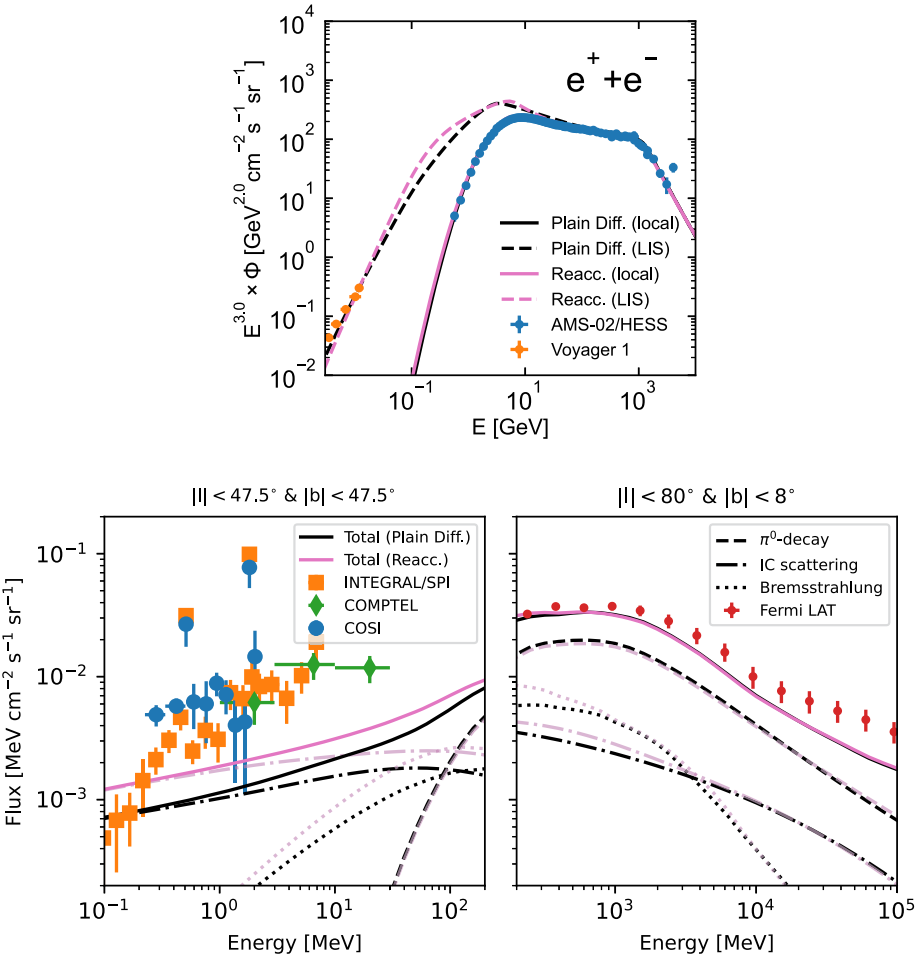

Fig. 2 *Upper panel:* Comparison of the locally observed primary CR electron + positron spectra by AMS-02 (Aguilar et al. 2014) and HESS (Aharonian et al. 2008) and the spectrum observed by Voyager-1 in interstellar space (Cummings et al. 2016) (denoted as "LIS" in panel legend) to expectations from two different models of CR propagation. Both models were computed with GALPROP (Porter et al. 2022), assuming plain diffusion + convection of CR in the ISM in one case (black), and diffusion with re-acceleration of CR in the ISM (pink) in the other case. *Lower panel:* Expected DGE emission in the MeV and GeV bands from the two CR propagation models shown in the upper panel. The expected emission (black/pink solid lines) is compared to the MeV observations displayed in Fig. 1, and to the measurement of the diffuse emission by *Fermi* LAT in Ackermann et al. (2012c) (red bars, right panel). *Fermi*-LAT measurements have been published for a different region of the sky than the MeV measurements in the left panel. The corresponding region is indicated above the respective panel. Individual contributions from various interaction processes are shown as dashed/dotted lines (see legend)

vection speed increasing with distance from the Galactic plane ($v_0 = 0$ km s^{-1}, $dv/dz = 10$ km s^{-1} kpc^{-1}). Plain diffusion has been shown to describe the Galactic synchrotron emission spectrum in the radio band better than models which assume (strong) re-acceleration of CR in the interstellar medium (Strong et al. 2011). The second model shown is one with moderate re-acceleration. Such models describe the light element (p, He) CR spectra best,

according to an extensive study of propagation parameters in Jóhannesson et al. (2016). Re-acceleration of CR in the ISM typically removes the necessity for a break in the rigidity dependence of the diffusion coefficient. Moderate re-acceleration also remains consistent with synchrotron observations (Orlando 2018). GALPROP configuration files for the two models shown in Fig. 2 can be found in Ackermann (2025).

Below few tens of MeV, the DGE is almost entirely produced from IC scattering of CR electrons and positrons with the ISRF. The strongest variations of the intensity of the DGE between the two propagation scenarios depicted in Fig. 2 are visible in this energy range. At higher energies, interactions of CR nuclei with the ISG resulting in the production of $\pi^0 \rightarrow \gamma\gamma$ strongly dominate the DGE. Bremsstrahlung from the interactions of CR electrons with the ISG remains subdominant in the entire MeV energy range, but contributes significantly to the total DGE from few MeV to few hundreds of MeV. The bremsstrahlung and pion-decay components are strongly correlated to the distribution of the ISG column density and, correspondingly, their intensity exhibits strong intensity variations over the sky on all scales. In contrast, the IC component shows smooth variations over the sky, determined by CR electron and radiation field densities along each line of sight (see, e.g., Orlando 2019). The kinematics of the pion decay lead to a characteristic steep spectrum for the pion-decay component below $\frac{1}{2}m_{\pi^0} \approx 67.5$ MeV (Stecker 1971), allowing to distinguish it from bremsstrahlung based on its spectral shape.

A precise measurement of the spectrum and spatial distribution of the DGE in the transition region between 10 MeV and 100 MeV is therefore crucial to disentangle the contributions from the different processes. The CR energies that are responsible for the DGE in this energy range are typically around few tens of MeV to few GeV, a range where local measurements of CR spectra do not reflect their local interstellar spectrum (LIS) due to strong and time-dependent solar modulation effects (Potgieter 2013). The Voyager measurements of LIS spectra are limited to $\lesssim 50$ MeV for electrons and $\lesssim 350$ MeV for protons (Cummings et al. 2016). Precise γ-ray measurements of the DGE can indirectly probe the LIS CR spectrum above this energy range, and therefore, as discussed above, provide important constraints on CR propagation models. This can also be seen in the upper panel of Fig. 2 where the two models displayed exhibit clear differences in the electron + positron spectrum in the range between few tens of MeV and few GeV, where solar modulation effects are strong and no direct LIS measurements are available. In addition, the strong dominance of IC scattering and pion decay at low and high energies, respectively, unlocks the potential to improve our understanding of the ISRF and ISG distributions based on measurements of the spatial distributions of the γ-ray emission.

The measurement itself, however, is challenging for various reasons. The key energy range between 10 MeV and 100 MeV needs hybrid instruments that combine a Compton telescope with a pair detection instrument, such as the proposed *newASTROGAM* (Berge et al. 2025) and *AMEGO-X* (Caputo et al. 2022) concepts. At energies above 10 MeV the effective area of typical Compton telescopes decreases rapidly due to the decreasing Compton cross section and increasing leakage of Compton photons, while maintaining an $\mathcal{O}(1^\circ)$ angular resolution (Caputo et al. 2022). The effective area of pair creation instruments increases with energy, but their angular resolution deteriorates quickly for energies below 100 MeV due to the increasing effects of multiple scattering of the electron-positron pairs in the detector material. Their angular resolution reaches $\mathcal{O}(10^\circ)$ below few tens of MeV (de Angelis et al. 2018).

However, good angular resolution is crucial for disentangling the DGE from the foreground of unresolved Galactic and background of extragalactic sources, as well as extended diffuse structures such as the *Fermi* Bubbles and Loop I discussed in Sect. 3. The upcoming *COSI* Compton telescope (Tomsick et al. 2023) will be an important first step forward.

COSI will allow to resolve fainter foreground sources with its unprecedented continuum sensitivity around 1 MeV in energy, yielding a higher accuracy estimate of the contribution of unresolved sources to the DGE. It will also improve the resolution of spatial variations in the continuum DGE in this energy range. A future hybrid Compton/Pair instrument with an energy range from sub-MeV to multiple GeV allows to study these sources and extended foregrounds over a wide energy range with good angular resolution and sensitivity below 10 MeV and above 100 MeV. These measurements will facilitate a high-confidence estimation of the foreground/background source contribution to the DGE also in the energy range between 10 MeV and 100 MeV, where it is hard to achieve both, good angular resolution and sensitivity, simultaneously.

Other important foregrounds and backgrounds comprise the IGRB (see also Sect. 4) and γ-rays from the Earth's atmosphere. The IGRB intensity can be distinguished from the DGE by its isotropic distribution over the sky, while the Earth's γ-ray emission is predominantly an issue in the Compton regime, since the Compton scattering angle can be large. Additional shielding by a thick active veto system or the rejection of large scattering angles can help to suppress the Earth's γ-ray background.

Exploring the spatial distribution of the DGE and correlations to ISRF and ISG requires an instrument with significantly higher effective areas in the MeV range than that of past and current generations of instruments. Around 100 MeV, the expected DGE intensity from pion decay and IC scattering towards the inner Galaxy is similar for both components, $\sim 2 \times 10^{-3}$ MeV cm^{-2} s^{-1} sr^{-1}, according to the model shown in Fig. 2. However, at the Galactic poles the DGE intensity is more than an order of magnitude lower for IC scattering (Orlando 2019) and for the pion decay component (Ackermann et al. 2012c). Therefore, an instrument with an extended source sensitivity of $\lesssim 10^{-4}$ MeV cm^{-2} s^{-1} sr^{-1} in the energy range between 10 MeV and 100 MeV, such as *newASTROGAM* (Berge et al. 2025) or other proposed instruments, is required to study the DGE variations over the entire sky.

3 *Fermi* Bubbles and Loop I

Fermi bubbles (FBs) (Su et al. 2010; Su and Finkbeiner 2012; Ackermann et al. 2014; Narayanan and Slatyer 2017; Herold and Malyshev 2019) and Loop I (Berkhuijsen et al. 1971; Wolleben 2007; Vidal et al. 2015; Ade et al. 2016; Shchekinov 2018; Dickinson 2018; Kataoka et al. 2018; Schulreich et al. 2018; Lallement 2023) are the largest extended sources in the γ-ray sky (apart from the Milky Way Galaxy itself and the isotropic γ-ray background). In spite of many multi-wavelength observations of these objects and a significant modeling effort for FBs (Zubovas et al. 2011; Cheng et al. 2011; Crocker and Aharonian 2011; Guo and Mathews 2012; Yang et al. 2013; Crocker et al. 2015; Yang et al. 2022) and Loop I (Berkhuijsen et al. 1971; Wolleben 2007; Vidal et al. 2015; Ade et al. 2016; Shchekinov 2018; Dickinson 2018; Kataoka et al. 2018; Schulreich et al. 2018) their origin is still under debate. In particular, Loop I was originally discovered in radio observations (Berkhuijsen et al. 1971). Models based on the radio data include a nearby supernova remnant (Berkhuijsen et al. 1971) or superbubbles (supershells) created by stellar winds and supernovae of the local Scorpio-Centaurus OB association (Wolleben 2007). The large size of Loop I on the sky is explained because the distance to the edges of the superbubble is comparable to the size of the superbubble itself. One of the main arguments in favor of a local origin of Loop I is the polarization of light from stars behind a synchrotron emitting region (Vidal et al. 2015; Dickinson 2018). A structure similar to the radio Loop I is also visible in the X-ray data, where it is often referred to as the North polar spur or, more recently,

the *eROSITA* bubbles (Predehl et al. 2020). The X-ray observations suggest, however, that the corresponding structure is located at a much larger distance than the local superbubble due to absorption of soft X-rays by the interstellar gas (Kataoka et al. 2013; Lallement et al. 2016; Gu et al. 2016; Lallement 2023). Another argument in favor of the GC origin of Loop I is depolarization of low-frequency *WMAP* and *Planck* maps close to the Galactic plane (Carretti et al. 2013; Vidal et al. 2015; Ade et al. 2016).

The FBs were discovered (Su et al. 2010) in the *Fermi*-LAT data after about a year and a half of operations of the *Fermi* satellite (Atwood et al. 2009). Their symmetrical distribution above and below the GC region suggests that the FBs are created by an activity in that region, such as a jet or an outflow from the supermassive black hole Sgr A*, the AGN scenario (Zubovas et al. 2011; Cheng et al. 2011; Guo and Mathews 2012; Yang et al. 2013; Sarkar et al. 2017; Yang et al. 2022; Sarkar et al. 2023), a star-burst activity near the GC (Lacki 2014), or regular star formation and supernovae explosions (Crocker and Aharonian 2011; Crocker et al. 2015; Sarkar et al. 2017). In the AGN outflow or starburst scenarios the FBs are inflated on the timescale of millions to tens of millions of years. In this case, the γ-ray emission is explained by inverse Compton scattering of high energy electrons with the ISRF. Provided that the γ-ray emission from the FBs is observed above 100 GeV, the required energy of electrons is about 1 TeV (Ackermann et al. 2014). These electrons have a cooling time of 1 Myr or less (Ackermann et al. 2014), which is much shorter than the timescale of formation of the FBs. In order to explain the γ-ray emission from the FBs, a re-acceleration of electrons is necessary (Mertsch and Sarkar 2011). The FBs can also be modeled as a persistent structure in the Galaxy supported by the star formation and supernovae explosions near the GC. In this case the γ-ray emission mechanism is typically attributed to interactions of hadronic CRs with gas, where the required density of CRs can be accumulated on timescales of hundreds of millions to billions of years (Crocker and Aharonian 2011; Crocker et al. 2015; Shimoda and Asano 2024). Related features in microwave (Finkbeiner 2004; Pietrobon et al. 2012; Ade et al. 2013) and radio (Carretti et al. 2013) wavelengths are explained due to the presence of (re-accelerated) secondary leptons (Crocker et al. 2015). For recent reviews of the FBs and the *eROSITA* bubbles/Loop I see Lallement (2023), Sarkar (2024).

Extrapolations to MeV energies of leptonic and hadronic models of γ-ray emission measured by the *Fermi* LAT (Ackermann et al. 2014) for the high-latitude FBs and Loop I are presented in Fig. 3. Both for the FBs and Loop I we exclude the Galactic plane within $|b| < 10°$. The corresponding CR proton and electron populations are modeled by power-law with exponential cutoff functions. The parameters of the models are presented in Table 1. The upper left plot shows models of the FBs assuming a magnetic field of 10 μG, which is similar to the magnetic field in the models that can explain both the γ-ray and microwave haze emissions (Ackermann et al. 2014). For comparison, we also show the models with a much smaller magnetic field of 2 μG. The dashed purple line shows the leptonic model of the γ-ray emission. In the leptonic model we do not take the energy loss into account, i.e., we model directly the spectrum of CR electrons inside the FBs. The band shows the 68% containment of the models taking into account statistical and systematic (added in quadrature) uncertainties of the measured FB spectrum (Ackermann et al. 2014). In the hadronic model (solid blue line) we take into account the γ-ray emission from the primary interactions of the CR protons with the ISG (orange dash dotted) and the IC (green sparse dash-dotted line) and bremsstrahlung (red dotted line) emission of the secondary leptons interacting with the ISRF and ISG, respectively. For the ISRF we use a volume averaged model from GALPROP (Porter et al. 2008; Vladimirov et al. 2011; Porter et al. 2017) based on Ref. (Freudenreich 1998). We assume an ISG density of 0.01 cm^{-3} (Ferrière et al. 2007).

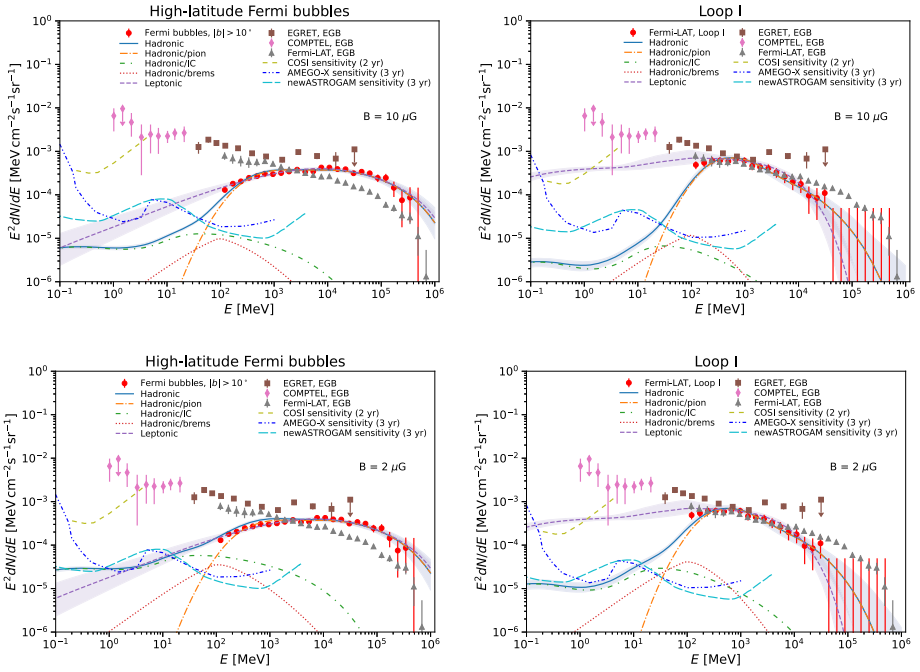

Fig. 3 Intensity of emission of the FBs (red circles, left panel) and Loop I (red circles, right panel) at latitudes $|b| > 10^{\circ}$ (Ackermann et al. 2014). Blue solid line shows the hadronic model of the γ-ray emission. Dashed orange line, green sparse dash-dotted line, and dotted red line show the primary π^0, secondary IC, and secondary bremsstrahlung components in the hadronic scenario respectively. Dashed purple line - leptonic scenario of γ-ray emission (dominated by IC emission). Bands show the 1 sigma model uncertainty ranges for statistical plus 10% systematic uncertainties in the data. Pink diamonds, brown squares, and grey upward triangles show the extragalactic diffuse γ-ray background measured by *COMPTEL* (Weidenspointner et al. 2000), *EGRET* (Strong et al. 2004), and *Fermi* LAT (Ackermann et al. 2015a) respectively. Yellow sparse dashed lines show expected *COSI* sensitivity after 2 years of observations (Tomsick et al. 2023) for an extended source with the area of the high-latitude FBs $\Omega \approx 1$ sr and Loop I $\Omega \approx 3$ sr respectively. Expected *AMEGO-X* (Caputo et al. 2022) and *newASTROGAM* (Berge et al. 2025) sensitivities for high-latitude FBs and Loop I after 3 years of observations are shown by blue dash-dot-dotted and cyan long-dashed lines respectively

With the 10 μG magnetic field and such an ISG density, the dominant energy loss for the secondary leptons is synchrotron radiation. As a result, one should expect the characteristic drop in the total γ-ray emission in the hadronic model below about 100 MeV (due to the mass of the π^0 meson). In the leptonic model, on the other hand, one can expect approximately a power-law extrapolation of the emission below 100 MeV. Consequently, the expected γ-ray emission between about 1 MeV and 100 MeV is lower in the hadronic model compared to the leptonic one. The derived predictions are generally consistent with previous estimates of the γ-ray emission from the FBs at MeV energies (de Angelis et al. 2018; Negro et al. 2022).

We show the expected sensitivity of *COSI* after 2 years of observations (Tomsick et al. 2023), *AMEGO-X* after 3 years (Kierans 2020), and *newASTROGAM* after 3 years (Berge et al. 2025) by yellow dashed, blue dash-dot-doted, and cyan long dashed lines respectively. The sensitivity for intensity of emission from an extended source is estimated from the point source (PS) flux sensitivity as follows. We assume that the PS flux sensitivity is dominated

Table 1 Parameters of the best-fit leptonic and hadronic models of the FBs and Loop I at $|b| > 10^\circ$ assuming two different values for the magnetic field $B = 2, 10\ \mu$G. The magnetic field only affects the secondary population of leptons in the hadronic model

Model	B (μG)	Index	$E_{\rm cut}$ (GeV)
FB hadronic	2, 10	2.06 ± 0.04	2200^{+1100}_{-750}
FB leptonic	2, 10	2.06 ± 0.18	970^{+320}_{-240}
Loop I hadronic	2	2.60 ± 0.15	350^{+980}_{-260}
Loop I hadronic	10	2.65 ± 0.13	460^{+1700}_{-360}
Loop I leptonic	2, 10	2.39 ± 0.28	21^{+11}_{-7}

by a solid angle $\Omega_{\rm PS} = \pi R^2$, where we use either 68% containment radius or the half maximum radius depending on the availability of the corresponding radii in the literature. We also assume that the background is proportional to the solid angle and that the statistical fluctuations in the background are proportional to the square root of the background, i.e., that the fluctuations satisfy Poisson statistics. Thus, we estimate the flux sensitivity for an extended source subtending a solid angle $\Omega_{\rm ext}$ as $F_{\rm ext} = F_{\rm PS}\sqrt{\Omega_{\rm ext}/\,\Omega_{\rm PS}}$. The corresponding sensitivity for intensity of emission is then $I_{\rm ext} = F_{\rm ext}/\,\Omega_{\rm ext} = F_{\rm PS}/\sqrt{\Omega_{\rm ext}\Omega_{\rm PS}}$. We note that since $F_{\rm PS} \propto \sqrt{\Omega_{\rm PS}}$ in the regime where the sensitivity is dominated by the background, $I_{\rm ext}$ does not depend on $\Omega_{\rm PS}$ as long as the size of the extended source is much larger than the PSF radius. For *newASTROGAM* and *AMEGO-X* we take $\Omega_{PS} = \pi R^2_{68\%}$. For *newASTROGAM*, we use a characteristic value of the 68% containment radius at 50 MeV of 4°, which is slightly larger than the corresponding radius for the *e-ASTROGAM* configuration (de Angelis et al. 2018). For *AMEGO-X*, we use the 68% containment radius of 5° at 50 MeV (Kierans 2020). For *COSI*, we use the half-width half-maximum radius of 2° (Tomsick et al. 2023). We find that for the 10 μG magnetic field, the difference between the leptonic and hadronic models can be detected by the *newASTROGAM* and *AMEGO-X* experiments in the energy range between about 20 and 100 MeV. This conclusion strongly depends on the assumption about the magnetic field. For a much smaller magnetic field of, e.g., 2 μG the hadronic model is practically indistinguishable from the leptonic model down to hundreds of keV, where the difference is at a sub-percent level compared to the isotropic diffuse background (cf. Fig. 4). Thus, a presence of a break in the spectrum below about 100 MeV is a strong support for the hadronic origin of the γ-ray emission. In the absence of a break below 100 MeV, an independent assessment of the magnetic field is necessary: for the magnetic fields on the order of 10 μG or above the leptonic model is preferred, while for much smaller magnetic fields than 10 μG both leptonic and hadronic models are possible.

The corresponding models for Loop I are shown in Fig. 3 on the right panels. The 10 μG and 2 μG cases are on the upper and lower panels, respectively. There is a break in the spectrum of the hadronic model below 100 MeV both for low and for high magnetic fields. The main reason is that the spectrum of the primary protons is softer in the Loop I case compared to the FBs (cf. Table 1), which results in a much smaller injected energy density of the secondary leptons in the Loop I case. As a result, even for the 2 μG magnetic field, the hadronic model is significantly below the extrapolation of the leptonic model at energies $E < 100$ MeV. Although leptonic models of γ-ray emission from Loop I are generally preferred, especially in the GC outflow models of Loop I, there is still a possibility that the γ-ray emission has hadronic origin (Kataoka et al. 2018), e.g., in the superbubble scenario (Wolleben 2007; Shchekinov 2018). In this case, the situation is similar to supernova remnants, where the protons and nuclei can be responsible for the majority of the γ-ray production, while electrons are responsible for the synchrotron radio emission. An observation of a drop in the γ-ray emission below 100 MeV would be a signature of a hadronic origin of

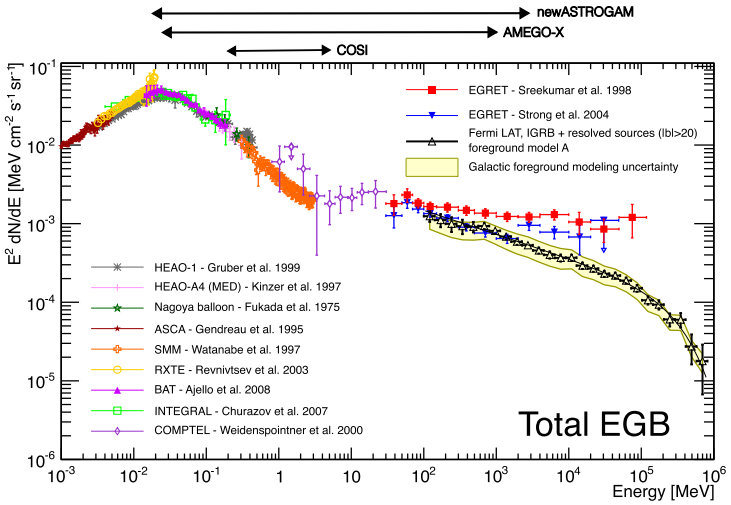

Fig. 4 Measurements of the extragalactic X-ray and γ-ray background from 1 keV to 820 GeV. The energy ranges of the upcoming *COSI* satellite and other proposed future γ-ray space missions are indicted by the arrows above the figure. Image reproduced with permission from Ackermann et al. (2015a), copyright by AAS

γ-ray emission from Loop I and an argument in favor of their local origin, although hadronic emission in Loop I in the GC outflow is also possible, e.g., (Kataoka et al. 2018). A flat SED below 100 MeV, on the other hand, would point to a leptonic origin of the γ-ray emission. In this case, both local and GC outflow models of Loop I are possible. Apart from Loop I, there are several other loops and spurs observed in radio data (Berkhuijsen et al. 1971; Vidal et al. 2015; Ade et al. 2016). At least one of these loops (Loop IV) is also detected in the γ-ray data (Jóhannesson and Porter 2021). Comparison of Loop I with the other loops may shed light on whether Loop I is a special feature or all loops have similar origin.

4 Extragalactic Diffuse Background

The first measurement of the MeV extragalactic background reaches all the way back to the *Apollo* missions (Trombka et al. 1977), which detected a diffuse emission component in the 0.3-10 MeV range with a high degree of isotropy. The existence of this cosmic radiation background was confirmed by *HEAO-1* (Kinzer et al. 1997), *SMM* (Watanabe et al. 1999b), *COMPTEL* (Weidenspointner et al. 2000), and other measurements in the MeV band. It was extended to GeV energies by *EGRET* (Sreekumar et al. 1998), and the most recent measurement above 100 MeV up to a maximum energy of 820 GeV was provided by the *Fermi* LAT (Ackermann et al. 2015a). Figure 4 provides a selection of measurements of the extragalactic X-ray and γ-ray background from 1 keV to 1 TeV.

A substantial fraction – if not all – of the IGRB emission is customarily attributed to unresolved sources from the various extragalactic γ-ray source populations. In the MeV to GeV energy range, emission from star-forming galaxies (SFGs) (Lacki et al. 2014), jetted and non-jetted active galactic nuclei (AGN), such as Seyfert galaxies (Inoue et al. 2008), radio galaxies (Inoue 2011), and blazars (Ajello et al. 2009), as well as the γ-ray emission from nuclear decays in cosmic supernovae, in particular SN Ia (Clayton and Ward 1975; Ruiz-Lapuente et al. 2016), all contribute to the IGRB.

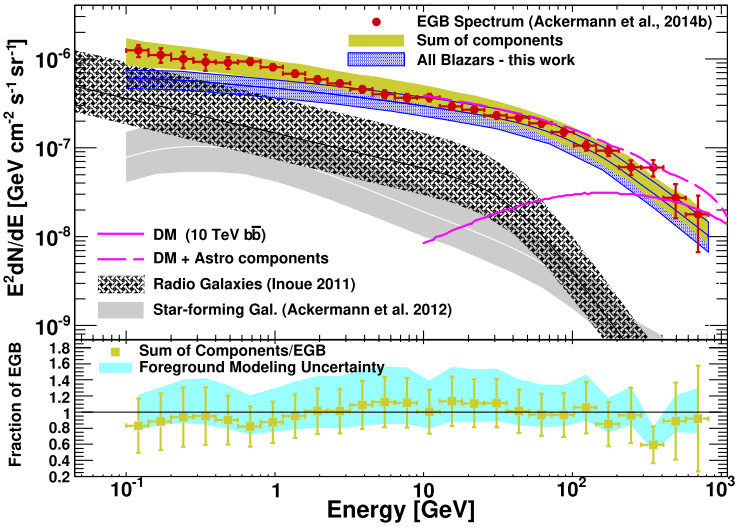

Fig. 5 Overview of the contributions of various source populations to the total EGB. The shaded areas represent the uncertainties in the contributions according to the calculations in the respective publications. The magenta line demonstrates how a potential γ-ray signal from dark matter annihilation would lead to features in the spectrum. Non-observation of such features allows to constrain the dark matter annihilation cross section. Image reproduced with permission from Ajello et al. (2015), copyright by AAS

While non-jetted AGN dominate the IGRB in the soft and hard X-ray range (Hasinger 2004), blazar emission is the dominant source of the IGRB above few tens of GeV (Ackermann et al. 2016). The fractional contributions of the various populations in the MeV and low GeV range is still under debate and one of the prime open questions of γ-ray astronomy. The energy range between few hundred keV and few tens of MeV might be dominated by Seyfert galaxies (Ananna et al. 2019) or blazars (Ajello et al. 2009), with unknown contributions from supernovae and jetted AGN (Ruiz-Lapuente et al. 2016). Apparent breaks in the IGRB spectrum at few MeV and few tens of MeV could be interpreted as an indication for the relevance of multiple source populations in this energy range. Existing measurements by *SMM* and *COMPTEL* do not constrain the IGRB spectrum enough to identify individual contributions based on their characteristic spectral shapes. However, the upcoming *COSI* satellite mission is expected to improve the precision of the spectral measurement significantly in the energy range between few hundred keV and few MeV. Starforming galaxies are expected to contribute significantly to the IGRB above few tens of MeV with widely varying predictions (e.g., Tamborra et al. 2014; Linden 2017; Ajello et al. 2020). A similar large range of predictions exists for the contribution of radio galaxies to the IGRB (e.g., Inoue 2011; Di Mauro et al. 2014; Hooper et al. 2016). Figure 5 shows a schematic overview of the contributions of various source populations to the EGB, based on calculations in Inoue (2011), Ackermann et al. (2012b), Ajello et al. (2015) and their quoted uncertainties.

Disentangling the various contributions depends on modeling of the γ-ray luminosity functions of the various populations and their spectral shapes in the energy range of interest. The obtained intensity can then be compared to the intensity of the total EGB. For most populations only few sources were detected with past and current instruments in the MeV range, too few to derive their luminosity functions directly. Consequently, observed or expected correlations between γ-ray luminosities and luminosities in other bands of the

electromagnetic spectrum are used to estimate the γ-ray luminosity functions, leading to a substantial statistical and systematic uncertainty (see, e.g., Inoue 2011; Ackermann et al. 2012b). Similarly, the spectral shape of sources is often interpolated from X rays and high-energy γ rays due to a lack of data in the MeV range.

Future γ-ray telescopes with improved sensitivity and angular resolution in the MeV range, will be able to advance our understanding of the IGRB in two ways. First, they will provide a more precise measurement of the IGRB and its spectral shape, due to their higher collection area and larger field-of-view. Second, they will allow to resolve a larger fraction of the total EGB into its individual source populations, providing a more direct measurement of their luminosity functions and spectral shapes.

The IGRB and total EGB are also of fundamental importance for searches for BSM physics. Since our Universe is transparent to γ rays, in particular in the MeV and low-GeV regimes, the γ-ray background provides strict constraints on the cumulative γ-ray emission from the observable Universe. This can be used to test, e.g., models of dark matter annihilation or decay (Ackermann et al. 2015b), or constrain the density of primordial black holes (Carr et al. 2010). Precise measurements and a detailed understanding of the IGRB are crucial to unleash the full potential of these searches that need to disentangle astrophysical contributions from unresolved sources and potential γ-ray emission from non-standard model particles and/or primordial black holes.

In multi-messenger astronomy, the EGB at MeV and GeV energies is a key observable due to is intrinsic connection to the extragalactic neutrino background (ENB) at TeV and PeV energies (Aartsen et al. 2020; Abbasi et al. 2022a) measured by the *IceCube* neutrino telescope (Aartsen et al. 2017). The ENB, much like the EGB, is considered to arise from unresolved neutrino sources.

The standard neutrino production process in astrophysical sources is the decay of charged pions produced in the interactions of nucleons with gas and photon targets in the local source environments. This process inevitably leads to the simultaneous production of high-energy photons (with similar energies as the neutrinos) from the decay of neutral pions generated in the same interactions. In contrast to neutrinos, TeV and PeV photons cannot propagate over cosmological distances, but interact with the extragalactic background light (EBL, e.g., Franceschini and Rodighiero 2017). Repeated pair production and IC interactions result in a cascading of the initial photons to GeV energies, at which the Universe is transparent for γ rays even at cosmological distances. This cascading in the EBL links the TeV/PeV neutrino background to the GeV γ-ray background and has been used to constrain properties of the neutrino sources and the neutrino spectrum below the energy range observable by *IceCube* (Murase and Waxman 2016).

Even more extreme cascading processes can alter the γ-ray spectra within the source environments close to the interaction region, e.g., within the photon targets that are producing the charged and neutral pions. In this case, intense UV to X-ray target photon fields would lead to a cascading even of GeV photons, which would finally escape at MeV energies. Such sources have been named "hidden" CR accelerators in Murase et al. (2016) since they might be invisible in the GeV band, and unobserved in the MeV band, where the sensitivity of current instruments trails sensitivities achieved for GeV γ rays. Remarkably, the first observation of a neutrino source, the Seyfert galaxy NGC 1068, shows a γ-ray luminosity in the GeV band that is more than an order of magnitude lower than its neutrino luminosity (Abbasi et al. 2022b), pointing to the described cascading in this source.

Models, such as (Murase 2022), of the broad-band emission of NGC 1068 consequently predict a strong emission in the MeV band, where the source becomes transparent to photons. The MeV γ-ray background holds the imprint of all such sources in the Universe and

can be used to constrain the population properties of "hidden" accelerators; in particular, in conjunction with the improved sensitivity of future MeV instruments and future neutrino telescopes that will allow to also individually detect the brightest of theses sources in γ rays and neutrinos.

The measurement of the isotropic γ-ray background is challenging for various reasons. Strong Galactic foregrounds lead to large systematic uncertainties in the determination of the IGRB in the GeV band (see Fig. 4). In the MeV band, the signal-to-noise between isotropic and Galactic gamma-ray emission improves significantly, however, new challenges arise: Secondary charged particles and γ rays produced by CRs in the Earth's atmosphere can mimic the isotropic γ-ray background. While a part of the background can be suppressed by active veto systems, some background remains irreducible, such as γ rays produced in secondary positron annihilation in passive material that inevitably surrounds any active shielding.

This secondary cosmic-ray contamination dominates the instrumental background for the IGRB measurement at few hundred MeV (Ackermann et al. 2012a). In addition, the fluxes of secondary charged particles with energies below few GeV in low-Earth orbit (LEO) are poorly measured (Mizuno et al. 2004; Cumani et al. 2019), leading to large systematic uncertainties in modeling the expected background. Future mission concepts should keep these challenges in mind when optimizing the design of the instrument and the orbit, e.g., by minimizing passive material outside of active veto systems and/or devising strategies to measure the secondary charged particle flux in-situ.

At tens of MeV, the Earth's albedo γ-ray emission and unresolved Galactic sources can become a significant background for the IGRB measurement. The quickly deteriorating PSF in pair-conversion telescopes (Ackermann et al. 2012a; de Angelis et al. 2018) at these energies leads to source confusion and makes it increasingly hard to reject the Earth emission. Below few MeV, a new background arises from the activation of spacecraft material due to CRs and trapped particles in orbit, leading to a significant increase in the instrumental background over time (Weidenspointner et al. 2001). Careful monitoring and modeling of this background is required to subtract it from the measured data. Again, choice of orbit, in particular avoiding the trapped particle populations in the South Atlantic Anomaly, and the design of the instrument can help to minimize this background.

5 Conclusions

Continuum diffuse γ-ray emission has been observed and studied since the early days of spaceflight that made their detection possible. Their main contributions, the DGE and the EGB are very different in nature. However, both contain essential clues for fundamental questions of physics and astronomy, such as the propagation of CRs in our Galaxy, or the nature of the non-baryonic matter in our Universe. Closely connected are large extended sources in the Milky Way, such as the FBs and Loop I, which have been observed from radio to GeV energies and provide unique information about the history of CR injection and high-power outflows in the Galaxy.

In this article we have demonstrated that a precise measurement of the spectrum and spatial distribution of the diffuse γ-ray emission in the MeV range is crucial for our ability to understand the origin of the emission. In the case of the DGE, this will allow us to separate the components that arise from interactions of CRs with the ISG and ISRF. It also will give us an independent handle on the LIS spectrum of CR electrons in an energy range where

local observations are dominated by solar modulation effects, but which is critical for testing different CR propagation scenarios.

In the case of the EGB, a precise measurement of its spectrum will help us to identify and quantify the contributions of the various source populations in the γ-ray sky, and constrain potential additional contributions, e.g., from the annihilation of dark matter particles or the evaporation of primordial black holes. In a multi-messenger approach it will also connect neutrino and γ-ray observations, and help in understanding the properties of high-energy neutrino sources.

In the case of extended sources, such as FBs and Loop I, high sensitivity in the MeV to hundred MeV range will allow one to distinguish in many scenarios leptonic and hadronic models of γ-ray production, which in turn will put constraints on the origin of these structures. In particular, leptonic models are favored in the AGN scenario of FB formation, while hadronic emission is generally preferred in scenarios involving star formation and supernovae.

The upcoming *COSI* satellite mission, covering the energy range from few hundred keV to few MeV with unprecedented sensitivity, is a crucial first step towards achieving the described advancements in our understanding of the origin of diffuse γ-ray emission and large extended structures in the γ-ray sky. Ultimately, it will, however, require a new generation of MeV telescopes, such as *newASTROGAM* or *AMEGO-X*, which are one to two orders of magnitude more sensitive than past and current instruments and cover a wide energy range from sub-MeV to low-GeV energies.

Funding Information Open Access funding enabled and organized by Projekt DEAL.

Declarations

Competing Interests All authors certify that they have no affiliations with or involvement in any organization or entity with any financial interest or non-financial interest in the subject matter or materials discussed in this manuscript.

References

Aartsen MG, Ackermann M, Adams J, et al (2017) The IceCube Neutrino Observatory: instrumentation and online systems. J Instrum 12(3):03012. https://doi.org/10.1088/1748-0221/12/03/P03012. arXiv:1612.05093 [astro-ph.IM]

Aartsen MG, Ackermann M, Adams J, et al (2020) Characteristics of the diffuse astrophysical electron and tau neutrino flux with six years of IceCube high energy cascade data. Phys Rev Lett 125(12):121104. https://doi.org/10.1103/PhysRevLett.125.121104

Abbasi R, Ackermann M, Adams J, et al (2022a) Improved characterization of the astrophysical muon-neutrino flux with 9.5 years of IceCube data. Astrophys J 928(1):50. https://doi.org/10.3847/1538-4357/ac4d29. arXiv:2111.10299 [astro-ph.HE]

Abbasi R, Ackermann M, Adams J, et al (2022b) Evidence for neutrino emission from the nearby active galaxy NGC 1068. Science 378(6619):538–543. https://doi.org/10.1126/science.abg3395. arXiv:2211.09972 [astro-ph.HE]

Abdo AA, Ackermann M, Ajello M, et al (2009) Fermi Large Area Telescope observations of the cosmic-ray induced γ-ray emission of the Earth's atmosphere. Phys Rev D 80(12):122004. https://doi.org/10.1103/PhysRevD.80.122004. arXiv:0912.1868 [astro-ph.HE]

Abdo AA, Ackermann M, Ajello M, et al (2011) Fermi Large Area Telescope observations of two gamma-ray emission components from the quiescent Sun. Astrophys J 734(2):116. https://doi.org/10.1088/0004-637X/734/2/116. arXiv:1104.2093 [astro-ph.HE]

Ackermann M (2025) Set of GALPROP v57 model definition files (used / for use in publications). Zenodo. https://doi.org/10.5281/zenodo.15007321

Ackermann M, Ajello M, Albert A, et al (2012a) The Fermi Large Area Telescope on orbit: event classification, instrument response functions, and calibration. Astrophys J Suppl Ser 203(1):4. https://doi.org/10.1088/0067-0049/203/1/4. arXiv:1206.1896 [astro-ph.IM]

Ackermann M, Ajello M, Allafort A, et al (2012b) GeV observations of star-forming galaxies with the Fermi Large Area Telescope. Astrophys J 755(2):164. https://doi.org/10.1088/0004-637X/755/2/164. arXiv:1206.1346 [astro-ph.HE]

Ackermann M, Ajello M, Atwood WB, et al (2012c) Fermi-LAT observations of the diffuse γ-ray emission: implications for cosmic rays and the interstellar medium. Astrophys J 750(1):3. https://doi.org/10.1088/0004-637X/750/1/3. arXiv:1202.4039 [astro-ph.HE]

Ackermann M, Albert A, Atwood WB, et al (2014) The spectrum and morphology of the Fermi Bubbles. Astrophys J 793(1):64. https://doi.org/10.1088/0004-637X/793/1/64. arXiv:1407.7905 [astro-ph.HE]

Ackermann M, Ajello M, Albert A, et al (2015a) The spectrum of isotropic diffuse gamma-ray emission between 100 MeV and 820 GeV. Astrophys J 799(1):86. https://doi.org/10.1088/0004-637X/799/1/86. arXiv:1410.3696 [astro-ph.HE]

Ackermann M, Ajello M, Albert A, et al (2015b) Limits on dark matter annihilation signals from the Fermi LAT 4-year measurement of the isotropic gamma-ray background. J Cosmol Astropart Phys 2015(9):008. https://doi.org/10.1088/1475-7516/2015/09/008. arXiv:1501.05464 [astro-ph.CO]

Ackermann M, Ajello M, Albert A, et al (2016) Resolving the extragalactic γ-ray background above 50 GeV with the Fermi Large Area Telescope. Phys Rev Lett 116(15):151105. https://doi.org/10.1103/PhysRevLett.116.151105. arXiv:1511.00693 [astro-ph.CO]

Ade PAR, Aghanim N, Arnaud M, et al (2013) Planck intermediate results. IX. Detection of the Galactic haze with Planck. Astron Astrophys 554:139. https://doi.org/10.1051/0004-6361/201220271. arXiv:1208.5483 [astro-ph.GA]

Ade PAR, Aghanim N, Alves MIR, et al (2016) Planck 2015 results. XXV. Diffuse low-frequency Galactic foregrounds. Astron Astrophys 594:25. https://doi.org/10.1051/0004-6361/201526803. arXiv:1506.06660 [astro-ph.GA]

Aguilar M, Aisa D, Alpat B, et al (2014) Precision measurement of the $(e^+ + e^-)$ flux in primary cosmic rays from 0.5 GeV to 1 TeV with the alpha magnetic spectrometer on the International Space Station. Phys Rev Lett 113(22):221102. https://doi.org/10.1103/PhysRevLett.113.221102

Aharonian F, Akhperjanian AG, Barres de Almeida U, et al (2008) Energy spectrum of cosmic-ray electrons at TeV energies. Phys Rev Lett 101(26):261104. https://doi.org/10.1103/PhysRevLett.101.261104. arXiv:0811.3894 [astro-ph]

Ajello M, Costamante L, Sambruna RM, et al (2009) The evolution of Swift/BAT blazars and the origin of the MeV background. Astrophys J 699(1):603–625. https://doi.org/10.1088/0004-637X/699/1/603. arXiv:0905.0472 [astro-ph.CO]

Ajello M, Gasparrini D, Sánchez-Conde M, et al (2015) The origin of the extragalactic gamma-ray background and implications for dark matter annihilation. Astrophys J 800(2):27. https://doi.org/10.1088/2041-8205/800/2/L27. arXiv:1501.05301 [astro-ph.HE]

Ajello M, Arimoto M, Axelsson M, et al (2019) A decade of gamma-ray bursts observed by Fermi-LAT: the second GRB catalog. Astrophys J 878(1):52. https://doi.org/10.3847/1538-4357/ab1d4e. arXiv:1906.11403 [astro-ph.HE]

Ajello M, Di Mauro M, Paliya VS, Garrappa S (2020) The γ-ray emission of star-forming galaxies. Astrophys J 894(2):88. https://doi.org/10.3847/1538-4357/ab86a6. arXiv:2003.05493 [astro-ph.GA]

Ananna TT, Treister E, Urry CM, et al (2019) The accretion history of AGNs. I. Supermassive black hole population synthesis model. Astrophys J 871(2):240. https://doi.org/10.3847/1538-4357/aafb77. arXiv:1810.02298 [astro-ph.GA]

Atwood WB, Abdo AA, Ackermann M, et al (2009) The Large Area Telescope on the Fermi gamma-ray space telescope mission. Astrophys J 697(2):1071. https://doi.org/10.1088/0004-637X/697/2/1071. arXiv:0902.1089 [astro-ph.IM]

Berezinskii VS, Smirnov AI (1975) Cosmic neutrinos of ultra high energies and detection possibility. Astrophys Space Sci 32(2):461–482. https://doi.org/10.1007/BF00643157

Berge D, Mazziotta MN, Tavani M, Tatischeff V, Oberlack U (2025) newASTROGAM – the New MeV to GeV Gamma-ray Observatory. arXiv e-prints. arXiv:2507.08133 [astro-ph.IM]

Bergström L, Edsjö J, Ullio P (2001) Spectral gamma-ray signatures of cosmological dark matter annihilations. Phys Rev Lett 87(25):251301. https://doi.org/10.1103/PhysRevLett.87.251301. arXiv:astro-ph/0105048 [astro-ph]
Berkhuijsen EM, Haslam CGT, Salter CJ (1971) Are the Galactic loops supernova remnants? Astron Astrophys 14:252
Berteaud J, Calore F, Iguaz J, Serpico PD, Siegert T (2022) Strong constraints on primordial black hole dark matter from 16 years of INTEGRAL/SPI observations. Phys Rev D 106(2):023030. https://doi.org/10.1103/PhysRevD.106.023030. arXiv:2202.07483 [astro-ph.HE]
Bignami GF, Boella G, Burger JJ, et al (1975) The COS-B experiment for gamma-ray astronomy. Space Sci Instrum 1:245–268
Bouchet L, Jourdain E, Roques J-P, et al (2008) INTEGRAL SPI all-sky view in soft gamma rays: a study of point-source and Galactic diffuse emission. Astrophys J 679(2):1315–1326. https://doi.org/10.1086/529489. arXiv:0801.2086 [astro-ph]
Bouchet L, Strong AW, Porter TA, et al (2011) Diffuse emission measurement with the SPectrometer on INTEGRAL as an indirect probe of cosmic-ray electrons and positrons. Astrophys J 739(1):29. https://doi.org/10.1088/0004-637X/739/1/29. arXiv:1107.0200 [astro-ph.HE]
Bouchet L, Jourdain E, Roques J-P (2015) The Galactic ^{26}Al emission map as revealed by INTEGRAL SPI. Astrophys J 801(2):142. https://doi.org/10.1088/0004-637X/801/2/142. arXiv:1501.05247 [astro-ph.HE]
Caputo R, Ajello M, Kierans CA, et al (2022) All-sky medium energy gamma-ray observatory eXplorer mission concept. J Astron Telesc Instrum Syst 8:044003. https://doi.org/10.1117/1.JATIS.8.4.044003. arXiv:2208.04990 [astro-ph.IM]
Carr BJ, Kohri K, Sendouda Y, Yokoyama J (2010) New cosmological constraints on primordial black holes. Phys Rev D 81(10):104019. https://doi.org/10.1103/PhysRevD.81.104019. arXiv:0912.5297 [astro-ph.CO]
Carr B, Kohri K, Sendouda Y, Yokoyama J (2021) Constraints on primordial black holes. Rep Prog Phys 84(11):116902. https://doi.org/10.1088/1361-6633/ac1e31. arXiv:2002.12778 [astro-ph.CO]
Carretti E, Crocker RM, Staveley-Smith L, Haverkorn M, Purcell C, Gaensler BM, Bernardi G, Kesteven MJ, Poppi S (2013) Giant magnetized outflows from the centre of the Milky Way. Nature 493(7430):66–69. https://doi.org/10.1038/nature11734. arXiv:1301.0512 [astro-ph.GA]
Cheng K-S, Chernyshov DO, Dogiel VA, Ko C-M, Ip W-H (2011) Origin of the Fermi Bubble. Astrophys J 731(1):17. https://doi.org/10.1088/2041-8205/731/1/L17. arXiv:1103.1002 [astro-ph.HE]
Clayton DD, Ward RA (1975) On emission lines in the cosmic gamma-ray background. Astrophys J 198:241–244. https://doi.org/10.1086/153599
Crocker RM, Aharonian F (2011) Fermi Bubbles giant, multibillion-year-old reservoirs of Galactic center cosmic rays. Phys Rev Lett 106(10):101102. https://doi.org/10.1103/PhysRevLett.106.101102. arXiv:1008.2658 [astro-ph.GA]
Crocker RM, Bicknell GV, Taylor AM, Carretti E (2015) A unified model of the Fermi Bubbles, microwave haze, and polarized radio lobes: reverse shocks in the Galactic center's giant outflows. Astrophys J 808(2):107. https://doi.org/10.1088/0004-637X/808/2/107. arXiv:1412.7510 [astro-ph.HE]
Cumani P, Hernanz M, Kiener J, Tatischeff V, Zoglauer A (2019) Background for a gamma-ray satellite on a low-Earth orbit. Exp Astron 47(3):273–302. https://doi.org/10.1007/s10686-019-09624-0. arXiv:1902.06944 [astro-ph.IM]
Cummings AC, Stone EC, Heikkila BC, et al (2016) Galactic cosmic rays in the local interstellar medium: Voyager 1 observations and model results. Astrophys J 831(1):18. https://doi.org/10.3847/0004-637X/831/1/18
de Angelis A, Tatischeff V, Grenier IA, et al (2018) Science with e-ASTROGAM. A space mission for MeV-GeV gamma-ray astrophysics. J High Energy Astrophys 19:1–106. https://doi.org/10.1016/j.jheap.2018.07.001. arXiv:1711.01265 [astro-ph.HE]
Di Mauro M, Calore F, Donato F, Ajello M, Latronico L (2014) Diffuse γ-ray emission from misaligned active Galactic nuclei. Astrophys J 780(2):161. https://doi.org/10.1088/0004-637X/780/2/161. arXiv:1304.0908 [astro-ph.HE]
Dickinson C (2018) Large-scale features of the radio sky and a model for Loop I. Galaxies 6(2):56. https://doi.org/10.3390/galaxies6020056
Diehl R, Dupraz C, Bennett K, et al (1995) COMPTEL observations of Galactic ^{26}Al emission. Astron Astrophys 298:445
Evoli C, Gaggero D, Vittino A, et al (2017) Cosmic-ray propagation with DRAGON2: I. numerical solver and astrophysical ingredients. J Cosmol Astropart Phys 2017(2):015. https://doi.org/10.1088/1475-7516/2017/02/015. arXiv:1607.07886 [astro-ph.HE]
Ferrière K, Gillard W, Jean P (2007) Spatial distribution of interstellar gas in the innermost 3 kpc of our Galaxy. Astron Astrophys 467(2):611–627. https://doi.org/10.1051/0004-6361:20066992. arXiv:astro-ph/0702532 [astro-ph]

Fichtel CE, Hartman RC, Kniffen DA, et al (1975) High-energy gamma-ray results from the second Small Astronomy Satellite. Astrophys J 198:163–182. https://doi.org/10.1086/153590
Finkbeiner DP (2004) Microwave interstellar medium emission observed by the Wilkinson Microwave Anisotropy Probe. Astrophys J 614(1):186. https://doi.org/10.1086/423482. arXiv:astro-ph/0311547 [astro-ph]
Franceschini A, Rodighiero G (2017) The extragalactic background light revisited and the cosmic photon-photon opacity. Astron Astrophys 603:34. https://doi.org/10.1051/0004-6361/201629684. arXiv:1705.10256 [astro-ph.HE]
Freudenreich HT (1998) A COBE model of the Galactic bar and disk. Astrophys J 492(2):495–510. https://doi.org/10.1086/305065. arXiv:astro-ph/9707340 [astro-ph]
Gu L, Mao J, Costantini E, Kaastra J (2016) Suzaku and XMM-Newton observations of the North polar spur: charge exchange or ISM absorption? Astron Astrophys 594:78. https://doi.org/10.1051/0004-6361/201628609. arXiv:1607.08334 [astro-ph.HE]
Guo F, Mathews WG (2012) The Fermi Bubbles. I. Possible evidence for recent AGN jet activity in the Galaxy. Astrophys J 756(2):181. https://doi.org/10.1088/0004-637X/756/2/181. arXiv:1103.0055 [astro-ph.HE]
Hasinger G (2004) The X-ray background and AGNs. Nucl Phys B, Proc Suppl 132:86–96. https://doi.org/10.1016/j.nuclphysbps.2004.04.127. arXiv:astro-ph/0310804 [astro-ph]
Herold L, Malyshev D (2019) Hard and bright gamma-ray emission at the base of the Fermi Bubbles. Astron Astrophys 625:110. https://doi.org/10.1051/0004-6361/201834670. arXiv:1904.01454 [astro-ph.HE]
Hooper D, Linden T, Lopez A (2016) Radio galaxies dominate the high-energy diffuse gamma-ray background. J Cosmol Astropart Phys 2016(8):019. https://doi.org/10.1088/1475-7516/2016/08/019. arXiv:1604.08505 [astro-ph.HE]
Hunter SD, Bertsch DL, Catelli JR, et al (1997) EGRET observations of the diffuse gamma-ray emission from the Galactic plane. Astrophys J 481(1):205–240. https://doi.org/10.1086/304012
Inoue Y (2011) Contribution of gamma-ray-loud radio galaxies' core emissions to the cosmic MeV and GeV gamma-ray background radiation. Astrophys J 733(1):66. https://doi.org/10.1088/0004-637X/733/1/66. arXiv:1103.3946 [astro-ph.HE]
Inoue Y, Totani T, Ueda Y (2008) The cosmic MeV gamma-ray background and hard X-ray spectra of active Galactic nuclei: implications for the origin of hot AGN coronae. Astrophys J 672(1):5. https://doi.org/10.1086/525848. arXiv:0709.3877 [astro-ph]
Jóhannesson G, Porter TA (2021) Signatures of recent cosmic-ray acceleration in the high-latitude gamma-ray sky. Astrophys J 917(1):30. https://doi.org/10.3847/1538-4357/ac01c9. arXiv:2104.13708 [astro-ph.HE]
Jóhannesson G, Ruiz de Austri R, Vincent AC, et al (2016) Bayesian analysis of cosmic ray propagation: evidence against homogeneous diffusion. Astrophys J 824(1):16. https://doi.org/10.3847/0004-637X/824/1/16. arXiv:1602.02243 [astro-ph.HE]
Johnson WN III, Haymes RC (1973) Detection of a gamma-ray spectral line from the Galactic-center region. Astrophys J 184:103–126. https://doi.org/10.1086/152309
Karwin CM, Siegert T, Beechert J, et al (2023) Probing the Galactic diffuse continuum emission with COSI. Astrophys J 959(2):90. https://doi.org/10.3847/1538-4357/ad04df. arXiv:2310.12206 [astro-ph.HE]
Kataoka J, Tahara M, Totani T, et al (2013) Suzaku observations of the diffuse X-ray emission across the Fermi Bubbles' edges. Astrophys J 779(1):57. https://doi.org/10.1088/0004-637X/779/1/57. arXiv:1310.3553 [astro-ph.HE]
Kataoka J, Sofue Y, Inoue Y, Akita M, Nakashima S, Totani T (2018) X-ray and gamma-ray observations of the Fermi Bubbles and NPS/Loop I structures. Galaxies 6(1):27. https://doi.org/10.3390/galaxies6010027. arXiv:1802.07463 [astro-ph.HE]
Kierans CA (2020) AMEGO: exploring the extreme multimessenger universe. In: den Herder J-WA, Nikzad S, Nakazawa K (eds) Space telescopes and instrumentation 2020: ultraviolet to gamma ray. Society of photo-optical instrumentation engineers (SPIE) conference series, vol 11444, 1144431. https://doi.org/10.1117/12.2562352
Kinzer RL, Jung GV, Gruber DE, et al (1997) Diffuse cosmic gamma radiation measured by HEAO 1. Astrophys J 475(1):361–372. https://doi.org/10.1086/303507
Kissmann R (2014) PICARD: a novel code for the Galactic cosmic ray propagation problem. Astropart Phys 55:37–50. https://doi.org/10.1016/j.astropartphys.2014.02.002. arXiv:1401.4035 [astro-ph.HE]
Kraushaar WL, Clark GW, Garmire GP, et al (1972) High-energy cosmic gamma-ray observations from the OSO-3 satellite. Astrophys J 177:341. https://doi.org/10.1086/151713
Lacki BC (2014) The Fermi Bubbles as starburst wind termination shocks. Mon Not R Astron Soc 444:39–43. https://doi.org/10.1093/mnrasl/slu107. arXiv:1304.6137 [astro-ph.HE]
Lacki BC, Horiuchi S, Beacom JF (2014) The star-forming Galaxy contribution to the cosmic MeV and GeV gamma-ray background. Astrophys J 786(1):40. https://doi.org/10.1088/0004-637X/786/1/40. arXiv:1206.0772 [astro-ph.HE]

Lallement R (2023) North polar spur/Loop I: gigantic outskirt of the Northern Fermi Bubble or nearby hot gas cavity blown by supernovae? C R Phys 23(S2):1–24. https://doi.org/10.5802/crphys.97. arXiv:2203.01312 [astro-ph.GA]
Lallement R, Snowden S, Kuntz KD, Dame TM, Koutroumpa D, Grenier I, Casandjian JM (2016) On the distance to the North polar spur and the local CO-H_2 factor. Astron Astrophys 595:131. https://doi.org/10.1051/0004-6361/201629453. arXiv:1609.03813 [astro-ph.GA]
Leventhal M, MacCallum CJ, Stang PD (1978) Detection of 511 keV positron annihilation radiation from the Galactic center direction. Astrophys J 225:11–14. https://doi.org/10.1086/182782
Linden T (2017) Star-forming galaxies significantly contribute to the isotropic gamma-ray background. Phys Rev D 96(8):083001. https://doi.org/10.1103/PhysRevD.96.083001. arXiv:1612.03175 [astro-ph.HE]
Luque PDlT, Balaji S, Silk J (2025) Anomalous ionization in the central molecular zone by sub-GeV dark matter. Phys Rev Lett 134(10):101001. https://doi.org/10.1103/PhysRevLett.134.101001. arXiv:2409.07515 [hep-ph]
Mertsch P, Sarkar S (2011) Fermi gamma-ray "bubbles" from stochastic acceleration of electrons. Phys Rev Lett 107(9):091101. https://doi.org/10.1103/PhysRevLett.107.091101. arXiv:1104.3585 [astro-ph.HE]
Mizuno T, Kamae T, Godfrey G, et al (2004) Cosmic-ray background flux model based on a gamma-ray large area space telescope balloon flight engineering model. Astrophys J 614(2):1113–1123. https://doi.org/10.1086/423801. arXiv:astro-ph/0406684 [astro-ph]
Murase K (2022) Hidden hearts of neutrino active galaxies. Astrophys J 941(1):17. https://doi.org/10.3847/2041-8213/aca53c. arXiv:2211.04460 [astro-ph.HE]
Murase K, Waxman E (2016) Constraining high-energy cosmic neutrino sources: implications and prospects. Phys Rev D 94(10):103006. https://doi.org/10.1103/PhysRevD.94.103006. arXiv:1607.01601 [astro-ph.HE]
Murase K, Guetta D, Ahlers M (2016) Hidden cosmic-ray accelerators as an origin of TeV-PeV cosmic neutrinos. Phys Rev Lett 116(7):071101. https://doi.org/10.1103/PhysRevLett.116.071101. arXiv:1509.00805 [astro-ph.HE]
Narayanan SA, Slatyer TR (2017) A latitude-dependent analysis of the leptonic hypothesis for the Fermi Bubbles. Mon Not R Astron Soc 468(3):3051–3070. https://doi.org/10.1093/mnras/stx577. arXiv:1603.06582 [astro-ph.HE]
Negro M, Fleischhack H, Zoglauer A, Digel S, Ajello M (2022) Unveiling the origin of the Fermi Bubbles with MeV photon telescopes. Astrophys J 927(2):225. https://doi.org/10.3847/1538-4357/ac5326. arXiv:2111.10362 [astro-ph.HE]
Orlando E (2018) Imprints of cosmic rays in multifrequency observations of the interstellar emission. Mon Not R Astron Soc 475(2):2724–2742. https://doi.org/10.1093/mnras/stx3280. arXiv:1712.07127 [astro-ph.HE]
Orlando E (2019) Implications on spatial models of interstellar gamma-ray inverse-Compton emission from synchrotron emission studies in radio and microwaves. Phys Rev D 99(4):043007. https://doi.org/10.1103/PhysRevD.99.043007. arXiv:1901.08604 [astro-ph.HE]
Orlando E, Strong AW (2008) Gamma-ray emission from the solar halo and disk: a study with EGRET data. Astron Astrophys 480(3):847–857. https://doi.org/10.1051/0004-6361:20078817. arXiv:0801.2178 [astro-ph]
Pietrobon D, Górski KM, Bartlett J, Banday AJ, Dobler G, Colombo LPL, Hildebrandt SR, Jewell JB, Pagano L, Rocha G, Eriksen HK, Saha R, Lawrence CR (2012) Analysis of WMAP 7 year temperature data: astrophysics of the Galactic haze. Astrophys J 755(1):69. https://doi.org/10.1088/0004-637X/755/1/69. arXiv:1110.5418 [astro-ph.GA]
Porter TA, Moskalenko IV, Strong AW, Orlando E, Bouchet L (2008) Inverse Compton origin of the hard X-ray and soft gamma-ray emission from the Galactic ridge. Astrophys J 682(1):400–407. https://doi.org/10.1086/589615. arXiv:0804.1774 [astro-ph]
Porter TA, Jóhannesson G, Moskalenko IV (2017) High-energy gamma rays from the Milky Way: three-dimensional spatial models for the cosmic-ray and radiation field densities in the interstellar medium. Astrophys J 846(1):67. https://doi.org/10.3847/1538-4357/aa844d. arXiv:1708.00816 [astro-ph.HE]
Porter TA, Jóhannesson G, Moskalenko IV (2022) The GALPROP cosmic-ray propagation and nonthermal emissions framework: release v57. Astrophys J Suppl Ser 262(1):30. https://doi.org/10.3847/1538-4365/ac80f6. arXiv:2112.12745 [astro-ph.HE]
Potgieter MS (2013) Solar modulation of cosmic rays. Living Rev Sol Phys 10(1):3. https://doi.org/10.12942/lrsp-2013-3. arXiv:1306.4421 [physics.space-ph]
Predehl P, Sunyaev RA, Becker W, et al (2020) Detection of large-scale X-ray bubbles in the Milky Way halo. Nature 588(7837):227–231. https://doi.org/10.1038/s41586-020-2979-0. arXiv:2012.05840 [astro-ph.GA]
Ruiz-Lapuente P, The L-S, Hartmann DH, et al (2016) The origin of the cosmic gamma-ray background in the MeV range. Astrophys J 820(2):142. https://doi.org/10.3847/0004-637X/820/2/142. arXiv:1502.06116 [astro-ph.HE]

Sarkar KC (2024) The Fermi/eROSITA Bubbles: a look into the nuclear outflow from the Milky Way. Astron Astrophys Rev 32(1):1. https://doi.org/10.1007/s00159-024-00152-1. arXiv:2403.09824 [astro-ph.HE]
Sarkar KC, Nath BB, Sharma P (2017) Clues to the origin of Fermi Bubbles from O viii/O vii line ratio. Mon Not R Astron Soc 467(3):3544–3555. https://doi.org/10.1093/mnras/stx314. arXiv:1610.00719 [astro-ph.GA]
Sarkar KC, Mondal S, Sharma P, Piran T (2023) Misaligned jets from Sgr A* and the origin of Fermi/eROSITA Bubbles. Astrophys J 951(1):36. https://doi.org/10.3847/1538-4357/acd75d. arXiv:2211.12967 [astro-ph.HE]
Schulreich MM, Breitschwerdt D, Feige J, Dettbarn C (2018) A way out of the bubble trouble?—upon reconstructing the origin of the local bubble and loop I via radioisotopic signatures on Earth. Galaxies 6(1):26. https://doi.org/10.3390/galaxies6010026. arXiv:1802.09275 [astro-ph.HE]
Shchekinov Y (2018) Multi-wavelength observations and modeling of Loop I. Galaxies 6(2):62. https://doi.org/10.3390/galaxies6020062
Shimoda J, Asano K (2024) Fermi and eROSITA Bubbles as persistent structures of the Milky Way. Astrophys J 973(2):78. https://doi.org/10.3847/1538-4357/ad6846. arXiv:2403.18474 [astro-ph.HE]
Siegert T, Boggs SE, Tomsick JA, et al (2020) Imaging the 511 keV positron annihilation sky with COSI. Astrophys J 897(1):45. https://doi.org/10.3847/1538-4357/ab9607. arXiv:2005.10950 [astro-ph.HE]
Siegert T, Berteaud J, Calore F, Serpico PD, Weinberger C (2022) Diffuse Galactic emission spectrum between 0.5 and 8.0 MeV. Astron Astrophys 660:130. https://doi.org/10.1051/0004-6361/202142639. arXiv:2202.04574 [astro-ph.HE]
Skibo JG, Johnson WN, Kurfess JD, et al (1997) OSSE observations of the soft gamma-ray continuum from the Galactic plane at longitude 95 degrees. Astrophys J 483(2):95–98. https://doi.org/10.1086/310755. arXiv:astro-ph/9704207 [astro-ph]
Sreekumar P, Bertsch DL, Dingus BL, et al (1998) EGRET observations of the extragalactic gamma-ray emission. Astrophys J 494(2):523–534. https://doi.org/10.1086/305222. arXiv:astro-ph/9709257 [astro-ph]
Stecker FW (1971) Cosmic gamma rays. NASA special publication, vol 249. NASA, Washington DC
Strong AW, Bennett K, Bloemen H, et al (1994) Diffuse continuum gamma rays from the Galaxy observed by COMPTEL. Astron Astrophys 292:82–91
Strong AW, Bloemen H, Diehl R, Hermsen W, Schönfelder V (1999) COMPTEL skymapping: a new approach using parallel computing. Astrophys Lett Commun 39:209. arXiv:astro-ph/9811211 [astro-ph]
Strong AW, Moskalenko IV, Reimer O (2004) A new determination of the extragalactic diffuse gamma-ray background from EGRET data. Astrophys J 613(2):956–961. https://doi.org/10.1086/423196. arXiv:astro-ph/0405441 [astro-ph]
Strong AW, Orlando E, Jaffe TR (2011) The interstellar cosmic-ray electron spectrum from synchrotron radiation and direct measurements. Astron Astrophys 534:54. https://doi.org/10.1051/0004-6361/201116828. arXiv:1108.4822 [astro-ph.HE]
Su M, Finkbeiner DP (2012) Evidence for gamma-ray jets in the Milky Way. Astrophys J 753(1):61. https://doi.org/10.1088/0004-637X/753/1/61. arXiv:1205.5852 [astro-ph.HE]
Su M, Slatyer TR, Finkbeiner DP (2010) Giant gamma-ray bubbles from Fermi-LAT: active Galactic nucleus activity or bipolar Galactic wind? Astrophys J 724(2):1044–1082. https://doi.org/10.1088/0004-637X/724/2/1044. arXiv:1005.5480 [astro-ph.HE]
Tamborra I, Ando S, Murase K (2014) Star-forming galaxies as the origin of diffuse high-energy backgrounds: gamma-ray and neutrino connections, and implications for starburst history. J Cosmol Astropart Phys 2014(9):043. https://doi.org/10.1088/1475-7516/2014/09/043. arXiv:1404.1189 [astro-ph.HE]
Tomsick JA, Boggs SE, Zoglauer A, et al (2023) The Compton Spectrometer and Imager. PoS ICRC2023:745. https://doi.org/10.22323/1.444.0745. arXiv e-prints. arXiv:2308.12362 [astro-ph.HE]
Trombka JI, Dyer CS, Evans LG, et al (1977) Reanalysis of the Apollo cosmic gamma-ray spectrum in the 0.3 to 10 MeV energy region. Astrophys J 212:925–935. https://doi.org/10.1086/155117
Tsuji N, Inoue Y, Yoneda H, Mukherjee R, Odaka H (2023) MeV gamma-ray source contribution to the inner Galactic diffuse emission. Astrophys J 943(1):48. https://doi.org/10.3847/1538-4357/acab69. arXiv:2212.05713 [astro-ph.HE]
Vidal M, Dickinson C, Davies RD, Leahy JP (2015) Polarized radio filaments outside the Galactic plane. Mon Not R Astron Soc 452(1):656–675. https://doi.org/10.1093/mnras/stv1328. arXiv:1410.4438 [astro-ph.GA]
Vladimirov AE, Digel SW, Jóhannesson G, Michelson PF, Moskalenko IV, Nolan PL, Orlando E, Porter TA, Strong AW (2011) GALPROP WebRun: an Internet-based service for calculating Galactic cosmic ray propagation and associated photon emissions. Comput Phys Commun 182(5):1156. https://doi.org/10.1016/j.cpc.2011.01.017. arXiv:1008.3642 [astro-ph.HE]
Wang W, Harris MJ, Diehl R, et al (2007) SPI observations of the diffuse ^{60}Fe emission in the Galaxy. Astron Astrophys 469(3):1005–1012. https://doi.org/10.1051/0004-6361:20066982. arXiv:0704.3895 [astro-ph]

Wang W, Siegert T, Dai ZG, et al (2020) Gamma-ray emission of ^{60}Fe and ^{26}Al radioactivity in our Galaxy. Astrophys J 889(2):169. https://doi.org/10.3847/1538-4357/ab6336. arXiv:1912.07874 [astro-ph.HE]

Watanabe K, Hartmann DH, Leising MD, The L-S (1999a) The diffuse gamma-ray background from supernovae. Astrophys J 516(1):285–296. https://doi.org/10.1086/307110. arXiv:astro-ph/9809197 [astro-ph]

Watanabe K, Leising M, Share G, Kinzer R (1999b) SMM measurement of the isotropic cosmic gamma-ray background. In: AAS/high energy astrophysics division #4, vol 4, 06–01

Weidenspointner G, Varendorff M, Kappadath SC, Bennett K, Bloemen H, Diehl R, Hermsen W, Lichti GG, Ryan J, Schönfelder V (2000) The cosmic diffuse gamma-ray background measured with COMPTEL. In: McConnell ML, Ryan JM (eds) The fifth Compton symposium. American institute of physics conference series, vol 510. AIP, Melville, pp 467–470. https://doi.org/10.1063/1.1307028

Weidenspointner G, Varendorff M, Oberlack U, et al (2001) The COMPTEL instrumental line background. Astron Astrophys 368:347–368. https://doi.org/10.1051/0004-6361:20000489. arXiv:astro-ph/0012332 [astro-ph]

Weidenspointner G, Skinner G, Jean P, et al (2008) An asymmetric distribution of positrons in the Galactic disk revealed by γ-rays. Nature 451(7175):159–162. https://doi.org/10.1038/nature06490

Wolleben M (2007) A new model for the Loop I (North polar spur) region. Astrophys J 664(1):349–356. https://doi.org/10.1086/518711. arXiv:0704.0276 [astro-ph]

Yang H-YK, Ruszkowski M, Zweibel E (2013) The Fermi Bubbles: gamma-ray, microwave and polarization signatures of leptonic AGN jets. Mon Not R Astron Soc 436(3):2734–2746. https://doi.org/10.1093/mnras/stt1772. arXiv:1307.3551 [astro-ph.GA]

Yang H-YK, Ruszkowski M, Zweibel EG (2022) Fermi and eROSITA Bubbles as relics of the past activity of the Galaxy's central black hole. Nat Astron 6:584–591. https://doi.org/10.1038/s41550-022-01618-x. arXiv:2203.02526 [astro-ph.HE]

Yusifov I, Küçük I (2004) Revisiting the radial distribution of pulsars in the Galaxy. Astron Astrophys 422:545–553. https://doi.org/10.1051/0004-6361:20040152. arXiv:astro-ph/0405559 [astro-ph]

Zubovas K, King AR, Nayakshin S (2011) The Milky Way's Fermi Bubbles: echoes of the last quasar outburst? Mon Not R Astron Soc 415:21–25. https://doi.org/10.1111/j.1745-3933.2011.01070.x. arXiv:1104.5443 [astro-ph.GA]